Available online at www.sciencedirect.com
SCIENCE DIRECT®
Renewable Energy 30 (2005) 2057–2073
RENEWABLE ENERGY
www.elsevier.com/locate/renene

Technical note

Augmentation of heat transfer coefficient by using 90° broken transverse ribs on absorber plate of solar air heater

M.M. Sahu[a], J.L. Bhagoria[b,*]

[a]*Mechanical Engineering Department, L.N.C.T., Bhopal, MP 462023, India*
[b]*Mechanical Engineering Department, M.A.N.I.T., Bhopal, MP 462007, India*

Received 13 August 2004; accepted 29 October 2004
Available online 30 May 2005

Abstract

An experimental investigation has been carried out to study the heat transfer coefficient by using 90° broken transverse ribs on absorber plate of a solar air heater; the roughened wall being heated while the remaining three walls are insulated. The roughened wall has roughness with pitch (P), ranging from 10–30 mm, height of the rib of 1.5 mm and duct aspect ratio of 8. The air flow rate corresponds to Reynolds number between 3000–12,000. The heat transfer results have been compared with those for smooth ducts under similar flow and thermal boundary condition to determine the thermal efficiency of solar air heater.

Keywords: Solar air heater; Heat transfer and 90° broken transverse ribs

1. Introduction

Solar collectors, in the system for the utilization of solar thermal energy, have the same central role as boilers and furnaces in conventional energy systems. All heat exchangers with provision for radiant input would qualify as solar collectors. Solar collectors

* Corresponding author.
E-mail address: palak_bh@yahoo.co.in (J.L. Bhagoria).

0960-1481/$ - see front matter © 2004 Elsevier Ltd. All rights reserved.
doi:10.1016/j.renene.2004.10.016

Nomenclature

A	area of absorber plate, m^2
A_{duct}	flow cross-section area = WH, m^2
A_o	throat area of orifice meter, m^2
A_p	plate heat transfer area, m^2
C_d	coefficient of discharge
C_p	specific heat, J/kg k
D	channel hydraulic diameter, m
D_p	inside dia of pipe, m
D_o	diameter of orifice of the orifice plate, m
H	depth of the duct, m
h	convective heat transfer coefficient, W/m^2 k
I	solar insolation, W/m^2
K	thermal conductivity of air, W/m k
L	test section length, m
M	mass flow rate, kg/s
Nu	Nusselt number
P	wire pitch
Q_a	useful heat gain, W
Re	Reynolds number
T_a, t_a	atmospheric temperature, °C
T_i, t_i	air inlet temperature, °C
T_{fav}	average flow temperature of air, °C
T_{oav}	average outlet temperature of air, °C
V	velocity of fluid in pipe, m/s
W	duct width, m
W/H	channel aspect ratio

Symbols

β	diameter ratio
η_{th}	thermal efficiency
ν	kinematic viscosity, m^2/s
ρ	density of air, kg/m^3
ρ_m	density of manometer fluid, kg/m^3

(air heaters) have low thermal efficiency because of low convective heat transfer coefficient between the air and absorber plate which leads higher temperature to the absorber plate causes maximum thermal losses to environment [1,4,8]. It has been found that the main thermal resistance to the convective heat transfer is due to the formation of boundary layer on the heat transferring surface. Efforts for enhancing heat transfer have been directed towards artificially destroying or disturbing this boundary layer. Artificial roughness in the form of wires and in various arrangements have been used to create

turbulence near the wall or to break the boundary layer [2,3]. Thus, the artificial roughness can employed for the enhancement of heat transfer coefficient between the absorber plate and air and thereby improving the thermal performance of solar air heater.

Sufficient information is available in the literature about heat transfer characteristics for flow in the roughened circular tubes and channels in the turbulent flow. In the case of circular wires, the heat transfer coefficient around the wires it self is very high and the roughness wire orientation i.e. pitch strongly affects the flow structure [3,4]. The 90° broken wire roughness increases the turbulence in the channel with this effect the heat transfer coefficient is increases [5]. Thus, the application of 90° broken wire ribs to a solar air heater is worth exploring. It has been, therefore, planned to investigate the effects for different pitch of 90° broken wire rib roughness on the enhancement of thermal performance of the solar air heater.

In the present experimental study, the range of parameters covered are Reynolds number ranging from 3000–12,000, pitch of ribs from 10–30 mm, roughness height 1.5 mm and aspect ratio of eight.

2. Outdoor experimental program

2.1. Experimental apparatus

A schematic diagram of experimental setup is shown in Fig. 1. The flow system consists of two entry section, test section and exit section and a centrifugal blower. The three sides of wooden walls the entire length of the duct have a smooth surface while the broad wall is roughened. An unheated entrance duct length of 177 mm is provided. A short entrance length has been chosen because for a roughened duct the thermally fully developed establishes in short length of 2 to 3 hydraulic diameters (D) [1,6]. A 353 mm long exit section is installed to remove any down stream effect on the test section. It may be noted that ASHRAE Standard 93–77 [7] recommends entry and exit length of 2.5 and 5WH, respectively, i.e. 177 and 353 mm, respectively, for the duct. The test section is of 1.5 m length. The top side of the heated test section carries about 1 mm thick G.I. plate with integral rib roughness on the lower side. The top side of the entry and exit lengths of the duct are covered with smooth face 6 mm thick plywood. The exit end of the duct is connected to a 53 mm diameter pipe provided with an orifice plate to a rectangular to circular transition piece. The air flow rate through the test unit has been regulated with the help of a control valve installed at the inlet of the blower.

Butt welded 0.36 mm copper-constantan thermocouples, calibrated against mercury thermometer of 0.1° centigrade least count, have been used for the temperature measurement. Six thermocouples have been affixed along the axial center line of the plate in holes drilled 0.5 mm deep into the back of the plate are used to measure variation of the plate temperature.

A 26.5 mm throat diameter orifice plate fitted in a 53 mm diameter pipe with inclined (1:5) U-tube manometer is used to measure the air flow rate.

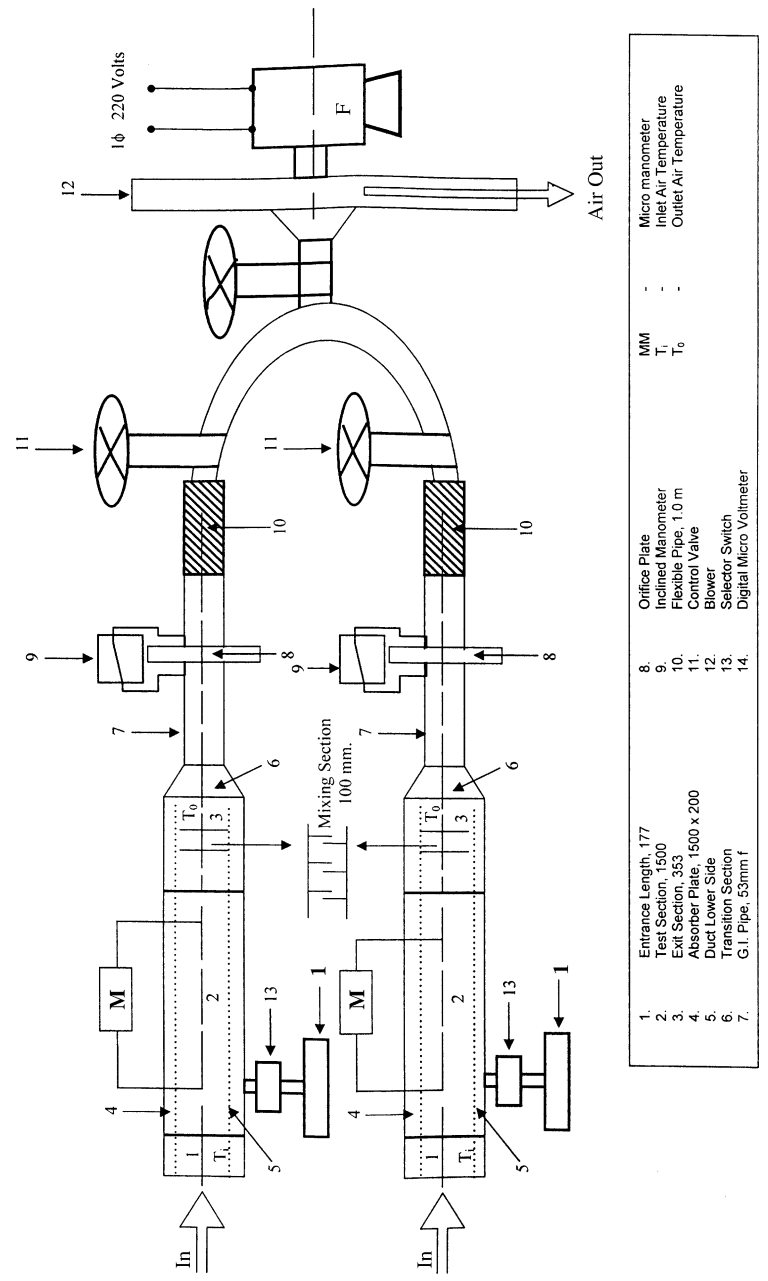

Fig. 1. Schematic diagram of experimental set up.

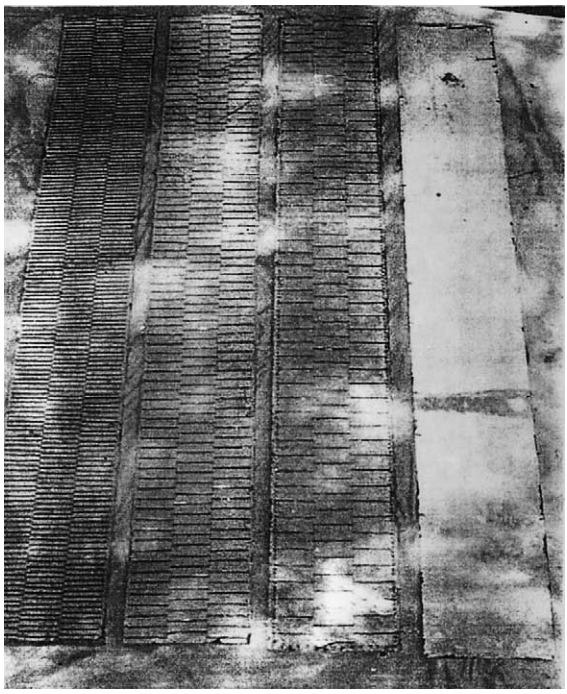

Fig. 2. Roughened absorber plates.

2.2. Absorber plates

The integral rib roughened G.I. absorber plates have been prepared by pasting circular wires of 1.5 mm diameter with different pitch over one side of the plate. Fig. 2 shows the geometry of the absorber plate with the 90° broken ribs. Some difficulties were experienced in getting plates manufactured to the exact dimensions. For the experiment four plates are used. One smooth and three were artificially roughened with roughness pitch of 10, 20 and 30 mm.

2.3. Experimental procedure

The test runs to collect the relevant heat transfer data were conducted under steady state conditions. Five values of flow rate were used for each set of tests. After each change of flow rate, the system was allowed to reach steady state before the data were recorded. The following parameters were measured:

1. Temperature of the heated plate and temperature of air at inlet and outlet of test section of the duct.
2. Pressure difference across orifice meter.
3. Solar insolation

Table 1
Experimental conditions

Parameter	Values
Reynolds number, Re	3000–12000
Channel aspect ratio, *W*/*H*	8.0
Test length, *L* (mm)	1500
Roughness height, *e* (mm)	1.5
Relative roughness height, *e*/*D*	0.0338
Hydraulic diameter, *D* (mm)	44.44
Roughness pitch (mm)	10, 20 and 30
Insolation, *I* (W/m^2)	750–880

3. Data reduction

3.1. Data analysis [1,8]

Table 1 shows the experimental parameter and Table 2–5 shows the experimental data for smooth and roughened duct.

3.1.1. Mean air and plate temperatures

The mean air temperature or average flow temperature T_{fav} is the simple arithmetic mean of the measure values at the inlet and exit of the test section. Thus,

$$T_{fav} = (T_i + T_{oav})/2 \tag{1}$$

The mean plate temperature, T_{pav} is the weighted average of the reading of six points located on the absorber plate.

3.1.2. Pressure drop calculation

Pressure drop measurement across the orifice plate was made by using the following relationship

$$\Delta P_0 = \Delta h \times 9.81 \times \rho_m \times 1/5 \tag{2}$$

where

ΔP_0, pressure diff.
ρ_m, density of the fluid
Δh, difference of liquid head in U-tube manometer.

3.1.3. Mass flow measurement

Mass flow rater of air has been determined from pressure drop measurement across the orifice plate by using the following relationship

$$m = C_d \times A_0[2 \times \rho \Delta P_0/(1 - \beta^4)]^{0.5}, \tag{3}$$

where

m, mass flow rate, Kg/s
C_d, coefficient of discharge of orifice i.e. 0.62

Table 2
Experimental data for smooth plate

S. no.	Reynolds number (Re)	Inlet temp. T_i (°C)	Avg. outlet temp. T_{oav} (°C)	Avg. fluid temp. T_{fav}(°C)	Avg. plate temp. T_{pav}(°C)	T_{oav}–T_i (°C)	T_{pav}–T_{fav} (°C)	Conv. heat transfer co. h (W/m^2 °C)	Nusselt number (Nu)	Thermal effi. η_{th} %
1	3000	39	62	50.5	129.5	23	79	6.571730	10.435865	58.99
2	5000	39.5	57	48.25	108.5	17.5	60	10.410556	16.631672	70.98
3	8000	40.5	51.5	46	89.5	11	43.5	14.738374	23.688766	72.85
4	10000	41	50	45.5	83	9	37.5	17.133333	27.57516	73.01
5	12000	41	48.5	44.75	78.75	7.5	34	19.070588	30.755131	73.67

Length of duct. = 1500 mm, width of duct. = 200 mm, height of duct. = 25 mm, e = 1.5 mm, e/D = 0.0338, α = 90°.

Table 3
Experimental data for roughened

S. no.	Reynolds number (Re)	Inlet temp. T_i (°C)	Avg. outlet temp. T_{oav} (°C)	Avg. fluid temp. T_{fav} (°C)	Avg. plate temp. T_{pav} (°C)	T_{oav}–T_i (°C)	T_{pav}–T_{fav} (°C)	Conv. heat transfer co. h (W/m^2 °C)	Nusselt number (Nu)	Thermal Effi η_{th}%
1	3000	40	60	50	125	20	75	6.019110	9.571300	51.29
2	5000	40.5	56.5	48.5	105	16	56	10.107960	16.137880	64.89
3	8000	41	51.7	46.1	85.9	10.7	39.8	15.670017	25.178998	70.87
4	10000	41	50	45.5	78	9	32.6	19.769230	31.817260	73.01
5	12000	40	47.5	43.75	72.25	7.5	28.5	22.750877	36.789899	73.68

PLATE (pitch = 10 mm), length of duct. = 1500 mm, width of duct. = 200 mm, height of duct. = 25 mm, e = 1.5 mm, e/D = 0.0338, α = 90°.

Table 4
Experimental data for roughened

S. no.	Reynolds number (Re)	Inlet temp. T_i (°C)	Avg. Outlet Temp. T_{oav}. (°C)	Avg. fluid temp. T_{fav} (°C)	Avg. plate temp. T_{Pav} (°C)	T_{oav}–T_i (°C)	T_{pav}–T_{fav} (°C)	Conv. heat transfer co. h (W/m^2 °C)	Nusselt number (Nu)	Thermal effi. η_{th} %
1	3000	40	65.5	52.75	136.75	25.5	84	6.849206	10.8121	65.4
2	5000	40	58.5	49.25	106	18.5	57.5	11.484060	18.2981	75.04
3	8000	41	53	47	87	12	37	18.900900	30.2971	79.47
4	10000	40.25	50.5	45.4	75.9	10.25	30.5	23.989071	38.6217	83.15
5	12000	40.25	48.75	44.5	72.25	8.5	27.75	26.481682	42.736	83.5

PLATE (pitch = 20 mm), length of duct. = 1500 mm, width of duct. = 200 mm, height of duct. = 25 mm, e = 1.5 mm, e/D = 0.0338, α = 90°.

Table 5
Experimental data for roughene

S. no.	Reynolds number (Re)	Inlet temp. T_i (°C)	Avg. outlet temp. T_{oav} (°C)	Avg. fluid temp. T_{fav} (°C)	Avg. plate temp. T_{pav} (°C)	T_{oav}–T_i (°C)	T_{pav}–T_{fav} (°C)	Conv. heat transfer co. h (W/m^2 °C)	Nusselt number (Nu)	Thermal effi. η_{th} %
1	3000	40	62	51	127	22	76	6.534211	10.363	56.4
2	5000	41	57.5	49.25	102.75	16.5	53.5	11.008720	17.5407	66.93
3	8000	41	52	46.5	83	11	36.5	17.566210	28.1956	72.85
4	10000	40.5	49.25	44.9	73	8.75	28.5	22.065450	35.5849	71.22
5	12000	40.5	47.25	43.9	68.9	7.25	25	25.072000	40.5433	71.22

PLATE (pitch = 30 mm), length of duct. = 1500 mm, width of duct. = 200 mm, height of duct. = 25 mm, e = 1.5 mm, e/D = 0.0338, α = 90°.

A_0, area of orifice plate, m^2
ρ, density of air i.e. 1.1415
β, ratio of dia. (d_0/D_p) i.e.26.5/53 = 0.5.

3.1.4. Velocity measurement

$$V = m/\rho WH \tag{4}$$

where
m, mass flow rate, Kg/s
ρ, density of air i.e. 1.1415 Kg/m^3
H, height of the duct, m (0.025)
W, width of duct, m (0.2).

3.1.5. Reynolds number

The Reynolds number for flow of air in the duct is calculated from:

$$\mathrm{Re} = V \times D/\nu, \tag{5}$$

$\nu = 16.7 \times 10^{-6}$ m^2/s
hydraulic diameter $D = 4WH/2(W+H)$.

3.1.6. Heat transfer coefficient

Heat transfer rate, Q_a, to the air is given by

$$Q_a = mC_p(T_0 - T_i) \tag{6}$$

The heat transfer coefficient for the heated test section has been calculated from

$$h = Q_a/A_p \times (T_{pav} - T_{fav}) \tag{7}$$

A_p is the heat transfer area assumed to be the corresponding smooth plate area.

3.1.7. Nusselt number

The heat transfer coefficient has been used the determine the Nusselt number and Stanton number defined as:

$$\mathrm{Nu} = hD/k \tag{8}$$

where k is the thermal conductivity of the air at the mean air temperature and D is the hydraulic diameter based on entire wetted parameter.

4. Results and discussion

The effect of various flow and roughness parameters on heat transfer characteristics for flow of air in rectangular ducts of different pitch in the present investigation are discussed below. Results have also been compared with those of smooth ducts under similar flow and geometrical conditions to see the enhancement in heat transfer coefficient. It can be seen

$y = -1E\text{-}07x^2 + 0.0051x - 4.171$ for Pitch = 20mm
$y = -6E\text{-}08x^2 + 0.0043x - 2.3086$ for Pitch = 30 mm
$y = -4E\text{-}08x^2 + 0.0036x - 0.9082$ for Pitch = 10 mm
$y = -1E\text{-}07x^2 + 0.0038x + 0.1366$ for Smooth Plate
Where x = Reynolds Number (Re) y = Nusselt Number (Nu)

e	=	1.5mm
α	=	90^0
W/H	=	8
D	=	44.44mm
I	=	880 W/m^2
e/D	=	0.0338

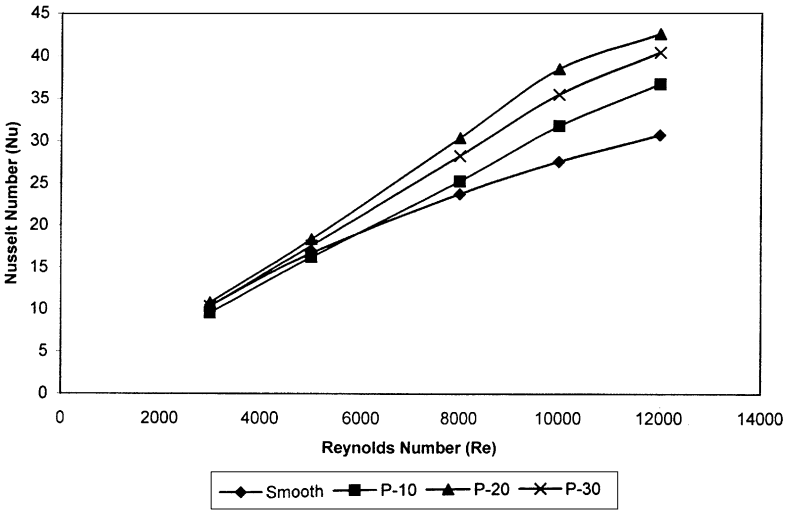

Plate / Re	3000	5000	8000	10000	12000
Smooth	10.43587	16.63167	23.68877	27.57516	30.75513
Pitch 10	9.57130	16.13788	25.17900	31.81726	36.78990
Pitch 20	10.81205	18.29807	30.29707	38.62168	42.73597
pitch 30	10.36295	17.54069	28.19557	35.58492	40.54333

Fig. 3. Variation for Nusselt number (Nu) with Reynolds number (Re)

from the Fig. 3, the values of Nusselt number increases with increases in Reynolds numbers. The Nusselt number was found maximum at the pitch value 20 mm, and increases, because it is nothing but the ratio of conductive resistance to convective resistance of heat flow and as Reynolds member increases thickness of boundary layer decreases and hence convective resistance decreases which in turn increases the Nusselt number.

It can be seen that for lower of Reynolds number, the improvement in the Nusselt number over the smooth duct is small. At very low Reynolds number (less than 5000), it can be seen from Fig. 3 that the value of Nusselt number for the smooth duct is nearly equal to that of rough duct may be attributed to the fact that the laminar sub layer thickness increases as the flow is retarded by roughness elements in Reynolds number region.

$y = -6E\text{-}08x^2 + 0.0032x - 2.4804$ for Pitch = 20 mm
$y = -4E\text{-}08x^2 + 0.0027x - 1.3799$ for Pitch = 30 mm
$y = -3E\text{-}08x^2 + 0.0023x - 0.5505$ for Pitch = 10 mm
$y = -6E\text{-}08x^2 + 0.0023x + 0.2032$ for Smooth Plate
Where x = Reynolds Number (Re) y = Conv. Heat Transfer Coeff. (h W/m^2 ^{0}C)

e	=	1.5mm
α	=	90^0
W/H	=	8
D	=	44.44mm
I	=	880 W/m^2
e/D	=	0.0338

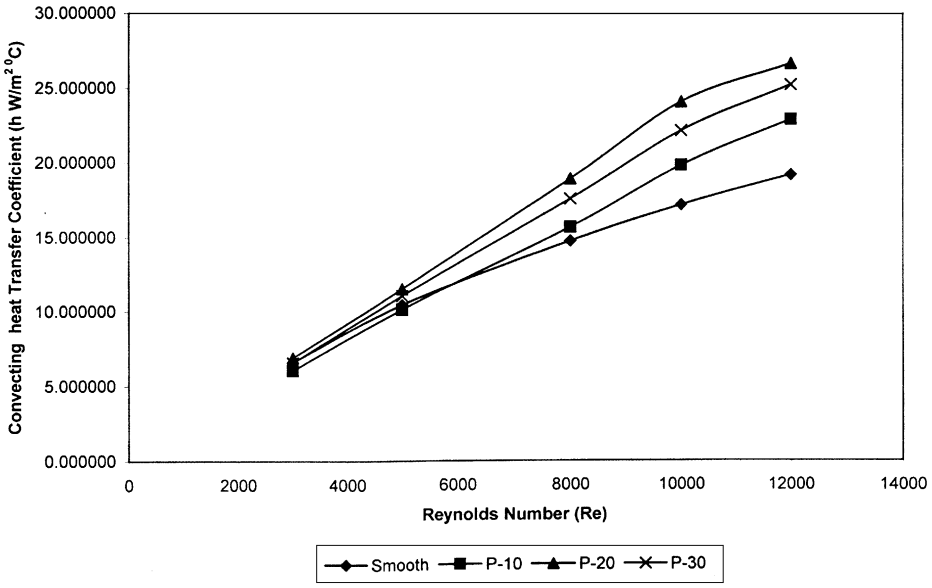

Plate / Re	3000	5000	8000	10000	12000
Smooth	6.57173	10.41056	14.73837	17.13333	19.07059
Pitch 10	6.01911	10.10796	15.67002	19.76923	22.75088
Pitch 20	6.84921	11.48406	18.90090	23.98907	26.48161
pitch 30	6.53421	11.00872	17.56621	22.06545	25.07200

Fig. 4. Variation of convective heat transfer coefficient (h, W/m^2 °C) with Reynolds number (Re).

As the Reynolds number increases heat transfer coefficient also increases for a constant values of pitch (Fig. 4). For low Reynolds number change in heat transfer coefficient is negligible with respect to roughness pitch, because when Reynolds number is low (<5000) the thermal boundary layer remains unbreakable, which offers resistance to heat flow and hence low heat transfer coefficient may result.

Fig. 5 shows the variation of Nusselt number with different pitch of 90° broken ribs. For various flow it can be seen from Fig. 5 that the Nusselt number values increases rapidly

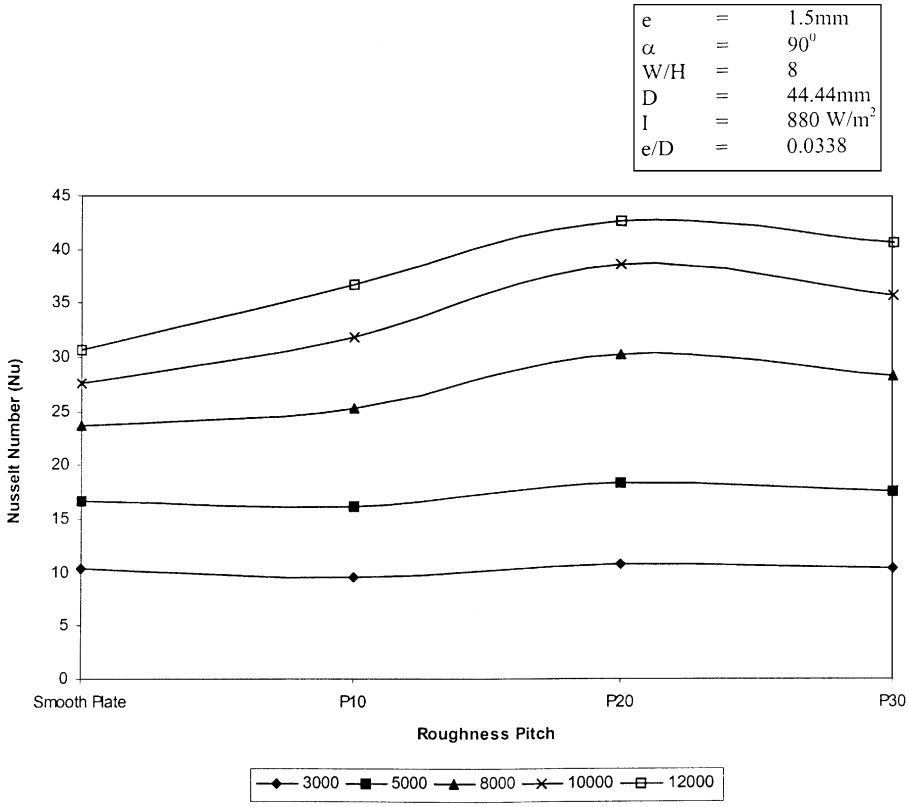

RE/PLATE	SMOOTH	PITCH = 10 mm	PITCH = 20mm	PITCH = 30mm
3000	10.43587	9.57130	10.81205	10.36295
5000	16.63167	16.13788	18.29807	17.54069
8000	23.68877	25.17900	30.29707	28.19557
10000	27.57516	31.81726	38.62168	35.58492
12000	30.75513	36.78990	42.73597	40.54333

Fig. 5. Variation of Nusselt number (Nu) with roughness pitch.

with increases in value of pitch up to 20 mm. Similarly it can also be seen in Fig. 6 that the value of convection heat transfer coefficient also increases rapidly with the value of pitch up to 20 mm. After that the rate of increases of Nusselt number and heat transfer coefficient decreases. In the case of low pitch value of 90° broken ribs, the reattachment point forms properly on the absorber plate surface. As the pitch increases the number of reattachment points decreases. So that at large pitch value (more than 20 mm) the number

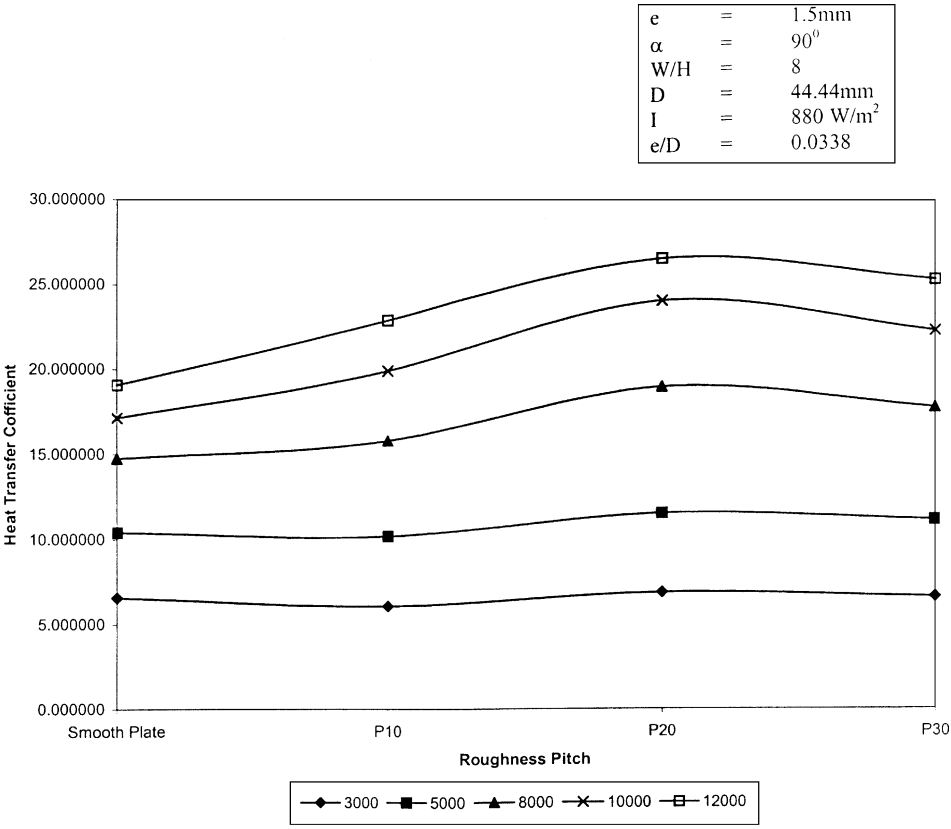

RE/PLATE	SMOOTH	PITCH = 10 mm	PITCH = 20mm	PITCH = 30mm
3000	6.57173	6.01911	6.84921	6.53421
5000	10.41056	10.10796	11.48406	11.00872
8000	14.73837	15.67000	18.9009	17.56621
10000	17.13333	19.76923	23.98907	22.06545
12000	19.07059	22.75088	26.48161	25.07200

Fig. 6. Variation of convective heat transfer coefficient (h, W/m^2 °C) with roughness pitch.

of reattachment points becomes less hence the heat transfer rate is decreases at higher pitch values. Similarly at low pitch value (less than 20 mm) due to the absence of reattachment point the heat transfer rate is low.

Airflow over 90° transverse ribs on a rib roughened wall separates at the top edges of the ribs. The flow reattaches in a region on the channel wall down stream of the ribs. A boundary layer and a reverse boundary layer develop in the region of reattachment

and grow in thickness in opposite directions. High heat transfer occurs in the vicinity of the reattachment region. Recirculation zones can be found adjacent to the upstream face, the down stream face and perhaps in some situations the top face of the rib.

For air flow over a staggered array of 90° broken ribs, separation occurs not only at the top edge of the rib but also at the edges at the end of the ribs, this secondary flow may also interrupt the growth of the boundary layer down stream of the nearby reattachment zones. This enhance the heat transfer coefficient in the 90° broken ribs, Fig. 7.

$y = -3E\text{-}07x^2 + 0.0057x + 51.36$ for Pitch = 20 mm
$y = -3E\text{-}07x^2 + 0.0063x + 44.53$ for Smooth Plate
$y = -4E\text{-}07x^2 + 0.0075x + 38.321$ for Pitch = 30 mm
$y = -4E\text{-}07x^2 + 0.0083x + 31.246$ for Pitch = 10 mm
Where x = Reynolds Number (Re) y = Thermal Efficiency (%)

e	=	1.5mm
α	=	90^0
W/H	=	8
D	=	44.44mm
I	=	880 W/m^2
e/D	=	0.0338

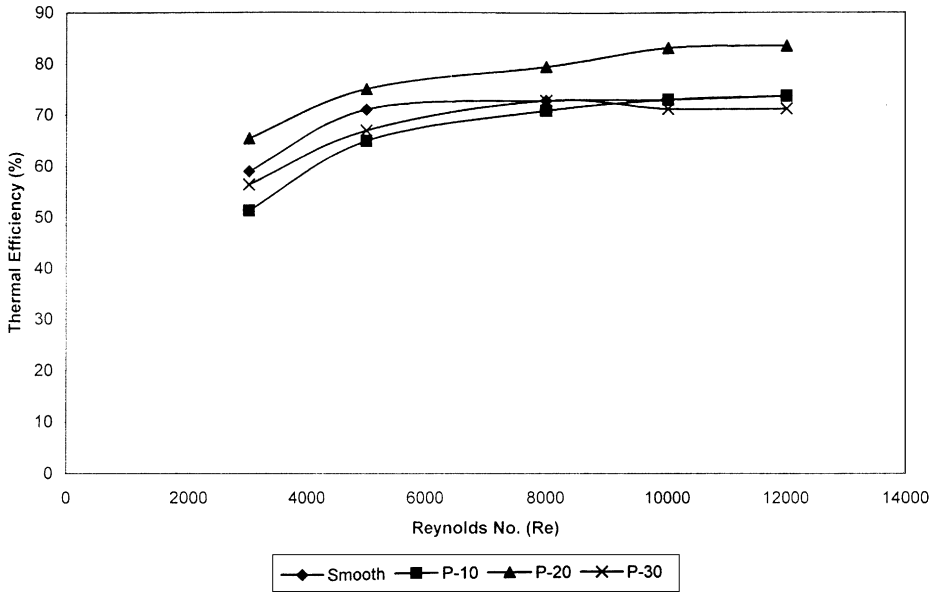

Plate / Re	3000	5000	8000	10000	12000
Smooth	58.99	70.98	72.85	73.01	73.67
Pitch 10	51.29	64.89	70.87	73.01	73.68
Pitch 20	65.4	75.04	79.47	83.15	83.5
pitch 30	56.4	66.93	72.85	71.22	71.22

Fig. 7. Variation of thermal efficiency (%) with Reynolds number (Re).

5. Conclusion

The present work was undertaken of with the objective of extensive investigation into broken 90° transverse ribs as artificial roughness on the undersides of one broad wall of solar air heater. Results have been compared with those of a smooth duct under similar flow conditions to determine enhancement in heat transfer coefficient and friction factor.

The following conclusions have been drawn from this investigation.

1. In the entire range of Reynolds number it is found that the Nusselt number increases, attains a maximum for roughness pitch of 20 mm and decreases with an increase of roughness pitch.
2. The value of the Nusselt number increases sharply at low Reynolds number and this becomes constant or increases very slightly in comparison to low Reynolds number This also satisfied our aim of solar collector application at low Reynolds number.
3. The maximum enhancement of heat transfer coefficient occurs at pitch of about 20 mm while on either side of this pitch the Nusselt number decreases.
4. It is also concluded that at low Reynolds number (below 5000) a smooth duct gives better heat transfer than the artificial roughened duct.
5. The experimental values of the thermal efficiency of the three roughened absorber plates tested have been compared with the smooth plates. A plate having roughness pitch 20 mm gives the highest efficiency of 83.5%.
6. In the field test on the solar heater with broken 90° ribs artificial roughness have been conducted to collect experiment data on thermal efficiency. Based on experimentation it is found that the maximum thermal efficiency of roughened solar air heater to of the order of (51–83.5%) depending upon the flow conditions.
7. Roughened absorber plates increase the heat transfer coefficient 1.25–1.4 times as compared to smooth rectangular duct under similar operating conditions at higher Reynolds number.

References

[1] Bhagoria JL. Heat transfer coefficient and friction factor correlations for rectangular solar air heater duct having transverse wedge shaped rib roughness oil the absorber plate. Int J Renewable Energy 2002;25: 341–69.
[2] Prasad K, Mullick SC. Heat transfer characteristics of a solar air heater used for drying purpose. Appl Energy 1985;12:83–93.
[3] Webb RL. Heat transfer and friction in tubes with repeated rib roughness. Int J Heat Mass Transfer 1971;14: 601–17.
[4] Prasad BN, Saini JS. Effect of artificial roughness on heat transfer and friction factor in solar air heater. Solar Energy 1988;41:555–60.
[5] Lau SC, Mc Millan RD, Han JC. J Turbomach Trans ASME 1991;113:360–6.
[6] Han JC, Park JS. Developing heat transfer in rectangular channels with rib trubulators. Int J Heat Transfer 1988;31:183–95.
[7] ASHARE standard 93–97, Method of testing to determine the thermal performance of solar collector, 1977.
[8] Sukhatme SP. Solar Energy. 4th.: Tata McGram Hill Publishing Company Limited; 1999. New Delhi Fourth Reprint.